

# Reconciling root plasticity and architectural ground rules in tree root growth models with voxel automata

Rachmat Mulia · Christian Dupraz ·  
Meine van Noordwijk

Received: 12 March 2010 / Accepted: 19 July 2010 / Published online: 12 August 2010  
© The Author(s) 2010. This article is published with open access at Springerlink.com

**Abstract** Dynamic models of tree root growth and function have to reconcile the architectural rules for coarse root topology with the dynamics of fine root growth (and decay) in order to predict the strategic plus opportunistic behaviour of a tree root system in a heterogeneous soil. We present an algorithm for a 3D model based on both local (soil voxel level) and global (tree level) controls of root growth, with development of structural roots as a consequence of fine root function, rather than as driver. The suggested allocation rules of carbon to fine root growth in each rooted voxel depend on the success in water uptake in this voxel during the previous day, relative to overall supply and demand at plant level. The allocated C in each voxel is then split into proliferation (within voxel growth) and extension into neighbouring voxels (colonisation), with scale-dependent thresholds and transfer coefficients. The fine

root colonisation process defines a dynamic and spatially explicit demand for transport functions. C allocation to development of a coarse root infrastructure linking all rooted voxels depends on the apparent need for adjustment of root diameter to meet the topologically defined sap flow through this voxel during the previous day. The allometric properties of the coarse root system are maintained to be in line with fractal branching theory. The model can predict the dynamics of the shape and structure (fine root density, coarse root topology and biomass) of the root system either independently of soil conditions (purely genetically-driven) or including both the genetic and environmental effects of roots interacting with soil water supply and its external replenishment, linking in with existing water balance models. Sensitivity of the initial model to voxel dimensions was addressed through explicit scaling rules resulting in scale-independent parameters. The model was parameterised for two tree species: hybrid walnut (*Juglans nigra* × *regia*) and wild cherry (*Prunus avium* L.) using results of a pot experiment. The model satisfactorily predicted the root growth behaviour of the two species. The model is sparse in parameters and yet applicable to heterogeneous soils, and could easily be upgraded to include additional local influences on root growth (and decay) such as local success in nutrient uptake or dynamic soil physical properties.

Responsible Editor: Alexia Stokes.

R. Mulia (✉) · M. van Noordwijk  
World Agroforestry Centre (ICRAF) SE Asia,  
P.O. Box 161, Bogor 16001, Indonesia  
e-mail: R.mulia@cgiar.org

M. van Noordwijk  
e-mail: M.vanNoordwijk@cgiar.org

C. Dupraz  
INRA, UMR-System,  
2 Place Viala, Building 27,  
34060 Montpellier Cedex 1, France  
e-mail: dupraz@supagro.inra.fr

**Keywords** Architecture · Coarse root · Fine root · Geotropism · Heterogeneous soil · Simulation model · Topology · Voxel automata

## Introduction

Plant productivity without either nutrient shortage (access issues) or losses affecting environmental quality (excess issues) depends on effective soil buffering, root distribution and activity (van Noordwijk and Cadisch 2002). Roots take up resources such as water and nutrients from heterogeneous soils (Hutchings and John 2004), responding to resource availability by activity and growth in relation to above ground demand. In intercropping systems or mixed vegetation, the potential uptake from different parts of the soil depends on the developing root system of competing plants, creating interacting feedback systems on root growth (van Noordwijk et al. 2004).

Through adaptive responses to heterogeneous environments, root systems may seem to take any shape, but transport functions and mechanical stability pose constraints. Plants have to reconcile plasticity with architectural ground rules, especially in woody perennials where long-distance transport in semi-permanent transport structures depends on more ephemeral fine root activity. Plant models ‘without roots’ can be adequate to relate available resources to uptake at field scale at a monthly or annual timescale. However, models that use spatial details of root distribution are required for accounts of competitive or resource-constrained systems and can be classified in four classes (Doussan et al. 2003; van Noordwijk and De Willigen 1986): a) models that ignore root dynamics and use time-independent root distributions, b) models that incorporate simple root dynamics described by a generic distribution model independent of both aboveground processes and soil conditions, c) models that simulate root system growth in response to conditions in the aboveground parts of the plant but without an interaction with soil environment, and iv) models that simulate the growth of a root system that senses and reacts to local soil conditions as well as to the conditions in the aboveground part of the plant. Currently, a number of root models of the four categories are available. Two approaches are available to describe the distribution of roots in the soil (Pagès et al. 2000). ‘Continuum’ type models usually describe root distribution relative to soil area or volume, e.g. as root length density. Architectural models represent root systems as a collection of root segments linked

in a topological structure. Some 3D architectural root models exist at level iv (e.g. Clausnitzer and Hopmans 1994; Diggle 1988; Dunbabin et al. 2002a, b; Somma et al. 1998). Many agronomical or forestry models at the plant scale need to link with a continuum root model for uptake functionality and with coarse root development as part of the C balance. To our knowledge, however, no 3D model for level iv has been developed using a continuum representation. Most continuum models were designed to simulate one-dimensional root growth (e.g. Asseng et al. 1997; Brugge and Thornley 1985; Grant 1989; Hayhoe 1981; Hillel and Talpaz 1976; Jones et al. 1991; Page and Gerwitz 1974). More recently, two-dimensional continuum root models have been proposed: root growth is modelled as a diffusion process (Acock and Pachepsky 1996; De Willigen et al. 2002; Heinen et al. 2003); some models constrain the root distribution by a negative exponential decrease with distance (vertically and laterally) from the plant base (Mobbs et al. 1999; van Noordwijk and Lusiana 2000). In the latter, the size (i.e. total mass or total length) of root system is dynamic over time but only the model of van Noordwijk and Lusiana (2000) takes into account dynamic responses to local soil conditions in a 2D frame.

Most of the above models do not simulate ‘coarse’ (often referred as structural) root growth as an important component of root systems to provide transport and mechanical stability. Yet the benefits to a plant of spreading fine roots over a large volume may be tempered by the disproportional ‘overhead’ costs of investment in transport infrastructure (van Noordwijk and Mulia 2002). Models of Mobbs et al. (1999) and van Noordwijk and Lusiana (2000) assume that total root biomass decreases according to a negative exponential distribution from the stembase proportional to the fine root system; but only in the latter, response of coarse root system to local soil conditions is considered. In this paper, we propose a model with continuum representation to simulate the growth of both fine and coarse root systems in 3D heterogeneous soil conditions. The model was designed with a 3D version of the cellular automata or the ‘voxel automata’ approach. Our purpose was to provide a generic and flexible root model that can be easily coupled with various process-based soil water balance models (in line with a level iv target)

and that can be used to test various hypotheses about the response of plant root systems to their environments, including in mixed cropping or agroforestry systems where the soil heterogeneity is induced by the competing rooting systems of various plants (Malézieux et al. 2008).

The objectives of this paper are: a) to describe a ‘teleonomic’ approach of modelling fine and coarse root system growth that reconciles root plasticity and architectural ground rules; b) to describe the parameter sensitivity to root patterns and shapes in an assumed permanent uniform soil water condition; c) to describe model parameterisation with two contrasting tree species; and iv) compare model performance with observations in a pilot experiment.

## Model description

### The continuous voxel automata

A voxel automaton is defined here as a discrete model that applies generic rules to an infinite, regular grid of voxels (volume elements in a three-dimensional grid). Time is handled in discrete time steps, and the state of a voxel at time  $t$  is a function of the state of a finite number of voxels called the neighbourhood at time  $t-1$ , potentially plus global time-dependent parameters. These neighbours are a selection of voxels defined by a transition rule. At each time step, the same transition rules are applied to the whole grid and a new generation is produced. The modelled process should be independent of the order of applying the transition rule to the voxels. In a continuous automaton, the state variables describing each voxel are continuous. The voxels and time-steps, however, remain discretely separated from each other.

We used a 3D continuous automaton to model the diffusive extension of a root system in the soil. The soil is partitioned into parallelepiped voxels identical in size. The root system is divided in two categories of roots: fine roots which are involved in the resource uptake mechanism and coarse roots that transport water and nutrients to aboveground parts of the plants, and provide mechanical stability. The operational distinction between fine and coarse roots is linked to model parameterisation rather than model structure; as default we used a threshold root diameter

of 2 mm: fine roots  $d < 2$  mm, coarse roots  $d > 2$  mm. Each voxel has two state variables: the fine root length density (FRLD,  $\text{m.m}^{-3}$ ) and the coarse root biomass density (CRBD,  $\text{g.m}^{-3}$ ). The neighbourhood of a voxel is defined as the six voxels that share a common face with the voxel (see below). The transition rules define how FRLD and CRBD change at the day time step, taking into account the neighbourhood information.

The root voxel automaton is under the forcing action of two input variables at the whole rooting system scale: the net daily supply of fine root dry matter (FRDM,  $\text{g day}^{-1}$ ) and the net daily supply of coarse root dry matter (CRDM,  $\text{g day}^{-1}$ ). These variables are either produced by the DM allocation module of a coupled plant model where the root automaton is embedded or estimated with experimental data. FRDM can be converted to root length using a specific root length (SRL,  $\text{m g}^{-1}$ ). Relative FRDM allocation to each rooted voxel is calculated as a function of the previous day contribution of the voxel to the total water extraction, and is split into proliferation (growth within the voxel) and colonisation (growth into neighbour voxels) (Fig. 1). Coarse root topology is deduced from the fine root colonisation paths, and CRDM is allocated to the various rooted voxels proportionally to the sap flow through the voxel during the previous day. A detailed explanation of root growth processes is given below. The six parameters used in the model are listed in Table 1.

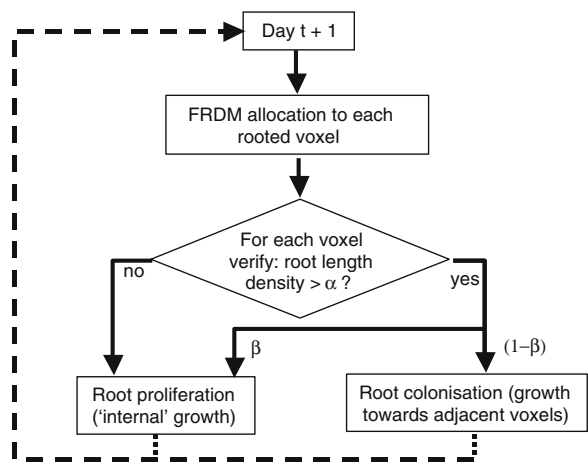


**Fig. 1** The universal voxel transition rule for fine roots included in the root automaton: balancing proliferation and colonisation

**Table 1** Six parameters used in the fine root voxel automaton governing fine root dry matter allocation to rooted voxels and root architecture

Parameter	Symbol and range	Unit
FRDM allocation to voxels		
○ Local water uptake factor	$-\infty < \varphi < +\infty$	–
○ Voxel-stembase topological distance factor	$-\infty < \rho < +\infty$	–
Root architecture		
○ Threshold of fine root colonisation	$\alpha \geq 0$	$\text{m m}^{-3}$
○ Proliferation rate (fraction of FRDM for proliferation)	$0 \leq \beta \leq 1$	–
○ Plagiotropism rate (fraction of colonisation to horizontal voxels)	$0 \leq \lambda \leq 1$	–
○ Geotropism rate (fraction of vertical colonisation to lower voxel)	$0 \leq \eta \leq 1$	–

### Allocation of FRDM input for local root growth

DM flux from a source to a sink depends on the source-sink distance and sink strength (Lacointe 2000; Le Roux et al. 2001). The latter depends on the potential growth rate of the sink, the local environmental conditions, or the previously achieved growth. We assume that the source of FRDM input is situated at the stembase and the fraction of the daily FRDM to each rooted voxel is a function of two factors: the local water uptake on the previous day and the voxel-stembase distance. The relative allocation to new fine roots in each voxel (x,y,z) at time t+1 is:

$$f_{x,y,z}^{\text{fr}}(t+1) = \frac{S_{x,y,z}(t)^{\varphi} D_{x,y,z}^{-\rho}}{\sum_1^n (S_{x',y',z'}(t)^{\varphi} D_{x',y',z'}^{-\rho})} \quad (1)$$

n is the number of rooted voxels.  $S_{x,y,z}(t)$  is the uptake of soil water (l) in day t in the (x,y,z) voxel. Positive  $\varphi$  values indicate that greater FRDM fractions are allocated to more successful voxels for water uptake. The null hypothesis (no impact of local water uptake on FRDM allocation) corresponds to  $\varphi=0$ ; negative  $\varphi$  values are mathematically possible but not physiologically meaningful.  $D_{x,y,z}$  is the topological distance from any voxel to the stembase, with  $\rho$  as a weighting factor (Balandier et al. 2000; Lacointe et al. 2002): positive and negative values of  $\rho$  indicate greater FRDM are allocated to proximal and distal voxels respectively. A zero value of  $\rho$  makes FRDM allocation independent of voxel-stembase distance. The topological distance between the voxel and the stembase  $D_{x,y,z}$  is calculated based on the model of self-generated coarse root topology (described below).

### Fine root proliferation and colonisation

The daily FRDM allowance is used for proliferation or extension into neighbouring voxels (colonisation). Root colonisation occurs only if the voxel root length density (RLD) is above a threshold value  $\alpha$ , representing the root biomass needed to reach across the voxel. Hayhoe (1981) estimated an  $\alpha$  value of  $3.0 \times 10^{-5} \text{ g cm}^{-3}$  for a maize root system whereas Grant (1989) used an  $\alpha$  value of  $2,500 \text{ m m}^{-3}$  ( $0.25 \text{ cm cm}^{-3}$ ) for the same crop species. With a typical SRL for fine roots of  $100 \text{ m g}^{-1}$  (van Noordwijk and Brouwer 1991) the Hayhoe value is equivalent to  $3,000 \text{ m m}^{-3}$ . The threshold is scaled with voxel volume.

Once the voxel RLD exceeds  $\alpha$ , the fraction  $\beta$  of the daily FRDM is used for proliferation, and  $(1-\beta)$  for colonisation. In their one-dimensional root model, Brugge and Thornley (1985) used a  $\beta$  value of 0.75 for a ryegrass root system with a standard layer thickness of 0.01 m. The  $\beta$  value, however, depends on dimensionality and scale. As simplification, the 3D colonisation process is assumed to concern only the six neighbour voxels that share a face with the 'parent-voxel' (i.e. the four horizontal, the upper and the lower voxels). The plagiotropism parameter  $\lambda$  describes the preference to perform horizontal rather than vertical colonisation and the geotropism parameter  $\eta$  splits the vertical colonisation between the lower (geotropism) and the upper neighbour (negative geotropism). The intensification of root colonisation from a parent-voxel to each of its four horizontal neighbour voxels is assumed to be proportional to the area of the shared face between each neighbour and the parent-voxel. The fractions of colonisation rate from a parent-voxel with

dimensions  $l_x$ ,  $l_y$ , and  $l_z$  in X, Y, and Z (vertical) directions are therefore:

$$f_{x+1,y,z}^{\text{col}} = f_{x-1,y,z}^{\text{col}} = 0.5 \frac{l_y}{l_x + l_y} (1 - \beta) \lambda \quad (2)$$

$$f_{x,y+1,z}^{\text{col}} = f_{x,y-1,z}^{\text{col}} = 0.5 \frac{l_x}{l_x + l_y} (1 - \beta) \lambda \quad (3)$$

$$f_{x,y,z+1}^{\text{col}} = (1 - \beta)(1 - \lambda)(1 - \eta) \quad (4)$$

$$f_{x,y,z-1}^{\text{col}} = (1 - \beta)(1 - \lambda) \eta \quad (5)$$

It can be verified that:

$$f_{x+1,y,z}^{\text{col}} + f_{x-1,y,z}^{\text{col}} + f_{x,y+1,z}^{\text{col}} + f_{x,y-1,z}^{\text{col}} + f_{x,y,z+1}^{\text{col}} + f_{x,y,z-1}^{\text{col}} = (1 - \beta) \quad (6)$$

Root colonisation is therefore assumed to be independent of the soil water conditions of the colonised voxels; the subsequent development of the ‘root colony’ however will depend on its own success in water extraction. Reciprocal root colonisation is allowed to occur among adjacent parent-voxels. Therefore, the actual increase in root length in a voxel will often be higher than its internal proliferation rate governed by  $\beta$ .

To avoid introducing artificial boundary effects, a 2D torus symmetry is applied: the finite computed scene is virtually surrounded by eight identical scenes. Each voxel situated on a vertical boundary is assumed to be the neighbour of the face-to-face boundary voxel. In the top and the bottom horizontal layer, each voxel has only five neighbours with a common face. No negative geotropism is allowed in the top voxel layer, and no geotropism in the bottom voxel layer.

Scaling parameters to adjust for variable voxel dimensions

If roots are assumed to be homogeneously distributed within a voxel,  $\beta$  and  $\lambda$  are dependent on voxel dimension, where  $\eta$  is not. A scaling rule is therefore introduced for the parameters to avoid any bias when

changing the voxels sizes. First of all, suppose that  $\beta$ ,  $\lambda$ , and  $\eta$  are FRDM transfer rates from a parent-voxel of dimension  $(l_x, l_y, l_z)$ . The fractions of roots that reach the neighbour voxels are described in Eqs. 2–5. If the length of the parent-voxel in x, y, and z direction are changed into  $L_x$ ,  $L_y$ , and  $L_z$  respectively then the fractions of roots that reach the six neighbours are linked to those of the original voxel as follows:

$$f_{x+1,y,z}^{\text{col}} = f_{x-1,y,z}^{\text{col}} = 0.5c \frac{(1 - \beta) \lambda l_x}{L_x} \quad (7)$$

$$f_{x,y+1,z}^{\text{col}} = f_{x,y-1,z}^{\text{col}} = 0.5(1 - c) \frac{(1 - \beta) \lambda l_y}{L_y} \quad (8)$$

$$f_{x,y,z+1}^{\text{col}} = \frac{(1 - \beta)(1 - \lambda)(1 - \eta) l_z}{L_z} \quad (9)$$

$$f_{x,y,z-1}^{\text{col}} = \frac{(1 - \beta)(1 - \lambda) \eta l_z}{L_z} \quad (10)$$

The constant  $c$  describes the shared faces between the horizontal neighbours and the parent voxel as described in Eqs. 2 and 3 by replacing  $l_x$  and  $l_y$  with  $L_x$  and  $L_y$  respectively. It can be noted that if  $L_x = l_x$ ,  $L_y = l_y$ , and  $L_z = l_z$  then Eqs. 7–10 becomes Eqs. 2–5.  $\beta$  as a function of voxel lengths (termed as effective  $\beta$ ) is derived from:

$$\beta^{\text{eff}} = 1 - f_{x+1,y,z}^{\text{col}} - f_{x-1,y,z}^{\text{col}} - f_{x,y+1,z}^{\text{col}} - f_{x,y-1,z}^{\text{col}} - f_{x,y,z+1}^{\text{col}} - f_{x,y,z-1}^{\text{col}} \quad (11)$$

To yield:

$$\beta^{\text{eff}} = 1 - (1 - \beta) \left( \frac{l_z}{L_z} + \lambda \left( \frac{c l_x}{L_x} + \frac{(1 - c) l_y}{L_y} - \frac{l_z}{L_z} \right) \right) \quad (12)$$

And this leads to effective  $\lambda$ :

$$\lambda^{\text{eff}} = 1 - \frac{(1 - \lambda) l_z}{l_z + \lambda L_z \left\{ \frac{c l_x}{L_x} + \frac{(1 - c) l_y}{L_y} - \frac{l_z}{L_z} \right\}} \quad (13)$$

A negative value of  $\beta^{\text{eff}}$  is possibly produced with Eq. 12 if  $L_x$ ,  $L_y$ , or  $L_z$  is less than  $l_x$ ,  $l_y$ , or  $l_z$

respectively. Only positive or zero values of  $\lambda^{\text{eff}}$  are produced with Eq. 13. Therefore, the scaling rule is valid for adapting the parameters to an increase of the voxel size, as compared to a reference size. The fractions of FRDM transferred from a parent voxel with a length of  $L_x$ ,  $L_y$ , and  $L_z$  m to its neighbours are therefore those of Eqs. 2–5 by replacing  $l_x$ ,  $l_y$ , and  $l_z$  with  $L_x$ ,  $L_y$ , and  $L_z$  respectively, and  $\beta$  and  $\lambda$  with  $\beta^{\text{eff}}$  and  $\lambda^{\text{eff}}$  respectively.

### Coarse root system growth and topology

The daily CRDM allocation to a voxel is proportional to the sap flow through the voxel during the previous day. The topology of the rooted system is required to calculate the sap flow of a parent-voxel as the sum of ‘internal’ water uptake plus those of its ‘offspring-voxels’ as follows:

$$G_{x,y,z}(t) = S_{x,y,z}(t) + \sum_1^k S_{x',y',z'}(t) \quad (14)$$

$G_{x,y,z}$  is the local flux of sap flow through the voxel (I).  $S_{x,y,z}$  is the local uptake of soil water; and  $k$  is the number of ‘up-stream’ voxels which have a topological link with the voxel. For voxels with no up-stream voxels (recently colonised voxels),  $G_{x,y,z} = S_{x,y,z}$ . A topological link between two voxels is created when fine roots of a parent voxel colonise an empty neighbour. However, to avoid anastomosis of the topology, a ‘one parent-voxel’ rule is applied. When several parent-voxels colonise an empty neighbour, only the most aggressive (i.e. with the highest FRDM allocation) is allowed to establish a topological link. If several parent-voxels provide exactly the same quantity of FRDM, a parent voxel is selected randomly. Coarse roots ‘appear’ in a voxel 2 days after an empty voxel has been colonised, as a consequence of Eq. 14. The topology algorithm also calculates voxel-stembase topological distance, as the sum of the distances between the centres of gravity of all the voxels along the topological pathway to the stembase.

### Root shapes in non-limiting soil water conditions

Possible genetically-determined root shapes generated by the automaton may be explored assuming homogeneous and permanent soil water availability in all

voxels. In such a condition, FRDM is proportional to root length density provided that potential water transport through the soil towards the roots is non-limiting and the internal resistance to water transport inside the coarse roots is negligible (van Noordwijk and Lusiana 2000). Theoretically,  $\alpha$  mainly determines the size of the rooted volume;  $\beta$  the gradient of the root length density within the rooted volume;  $\lambda$  the shape (width:depth ratio); and  $\eta$  the deepness of a rooting system.

The sensitivity of the model to  $\alpha$  and  $\beta$  was explored, with five values of  $\alpha$  (1,000 m m<sup>-3</sup> to 5,000 m m<sup>-3</sup> with 1,000 m m<sup>-3</sup> intervals) and six values of  $\beta$  (0 to 1 with 0.2 intervals). The effects on the size of the rooted volume and the gradient of root density were examined. The model was also run with six values of  $\lambda$  and  $\eta$  (0 to 1 with 0.2 intervals) to assess their contributions in determining the deepness of the rooting system.

### Sensitivity of the model outputs to the voxel dimension

The effect of the voxel dimension on the predicted rooting pattern was explored by comparing resulting root distribution profiles with different scene compartmentalisations. The same scene was compartmentalised in four different ways namely: a) 10 cm × 10 cm × 10 cm (in x, y, z direction respectively) small cubic voxels, b) 10 cm × 10 cm × 30 cm thick voxels, c) 30 cm × 30 cm × 10 cm flat voxels, or d) 30 cm × 30 cm × 30 cm large cubic voxels. The reference root distribution profile was assumed to be obtained with the first scenario. In the other scenario with larger voxels, the simulations were done with or without adjusted  $\beta$  and  $\lambda$  values.

### Model parameterisation

The model was parameterised using the results of a pot experiment carried out in 2003 at INRA Montpellier, France (Latitude 43° 35' 00" N and Longitude 03° 57' 41" E, altitude 54 m a.s.l.). The site has a sub-humid Mediterranean climate with an average daily temperature of 15°C and a total rainfall of 1,067 mm in 2003. A low rainfall total of 71 mm was observed during the tree growing months from May to August. The experiment consisted in growing tree seedlings in uniform soil conditions for penetrability, soil water



and nutrient content to monitor the 3D behaviour of rooting system in a homogeneous soil condition. It involved hybrid walnut (*Juglans nigra* × *regia*) and wild cherry (*Prunus avium* L.) trees. Both tree species are deciduous.

Tree seedlings aged 1 year were used and each tree was planted in a pot with a top and bottom diameter of 60 cm and 50 cm respectively, and 50 cm height ( $\approx 120$  l volume). We used pure perlite (i.e. expanded clay) which contains no nutritive elements. The physical and initial chemical characteristics of perlite are perfectly homogeneous. Roots can easily penetrate granules of perlite so that they can grow in every direction without any physical obstacle. Each pot was divided into four horizontal layers of 12.5 cm thickness separated by plastic grids of 2 cm × 2 cm mesh size. The grids were used for the ease of root harvesting without impeding root growth. Before plantation, root system of each tree was formatted to have a rooted volume of 10 cm × 10 cm and 25 cm depth. Each tree was planted in the middle of the pot and thus had initial root system situated in the two upper layers. Any root outside the 10 × 10 × 25 cm initial rooted volume observed at the harvesting period would represent new growth. There were 11 replications per species. Daily irrigation of water and a nutritive solution was carried out slowly and evenly distributed over the soil surface to maintain non-limiting and homogeneous soil water and nutrient conditions.

Due to a regular and uniform irrigation and fertilisation, we assumed that the trees grown in the perlite experiment experienced no gradients of soil resources. Under such a condition, the observed 3D root distribution patterns could reflect the role of parameters that determine root architecture, i.e. the two balancing proliferation and colonisation ( $\alpha$  and  $\beta$ ) and the two describing the preferential colonisation directions ( $\lambda$  and  $\eta$ ). Roots inside pots of perlite were collected voxel by voxel with 10 cm × 10 cm and 12.5 cm thickness at four times in the growing season (May, June, August, and October). There were 21 voxels per horizontal layers and 84 voxels per pot. Due to the circular form of the pots, the voxel configuration does not include areas near the lateral pot border. Tree roots found in these locations or found at the bottom of the pot were separated from those collected within the voxels. Two or three trees per species were harvested at each sampling date.

Fine ( $d < 2$  mm) and coarse ( $d > 2$  mm) roots were sorted in each voxel and the density was measured for the two root types. For model parameterisation, we used data of root density measured in the last harvesting date when the two species showed different spatial rooting patterns.

## Results

### Sensitivity of the predicted fine root patterns to the automaton parameters

The simulation results are synthesised by three indicators: (a) the index of extensiveness indicates the proportion of rooted voxels in the simulation scene; (b) the index of gradient reflects the ratio between standard deviation of root length density obtained with any  $\beta$  value relative to that obtained when  $\beta = 0$ ; and (c) the index of deepness measures the proportion of total fine root in deep horizontal layers. A very extensive root system will require both low values of  $\alpha$  and  $\beta$  (Fig. 2a). Both parameters have an important effect on the size of the rooted volume: the index of extensiveness decreases rapidly with the increase of  $\beta$  when  $\alpha$  is weak (e.g. from 60% to 42% with  $\alpha = 1,000 \text{ mm}^{-3}$ ) and with the increase of  $\alpha$  when  $\beta$  is weak (e.g. from 60% to 35% with  $\beta = 0$ ). Strong gradients of fine root density are generated with a combination of both high  $\alpha$  and  $\beta$  values (Fig. 2b). Deep rooting systems are obtained with low  $\lambda$  and high  $\eta$  value and both parameters have a significant effect (Fig. 2c).

### Corrected $\beta$ and $\lambda$ to adjust for larger voxels

The proliferation rate is increased with larger voxel sizes (Fig. 3a). It may not however approach a unit value when voxel lengths are increased in one or two directions only. If all voxel dimensions are increased in the same proportion (inflated cube), the  $\beta$  can reach 0.95 for a 25-fold increase. A lower  $\alpha$  is required with larger voxel lengths in horizontal directions (Fig. 3b). Conversely, if only the vertical dimension is increased,  $\lambda$  would approach a unit value indicating that a reduced vertical root colonisation is necessary to maintain the same root pattern. Interestingly, if all the voxel lengths are increased in the same way, the initial value of  $\lambda$  remains valid.

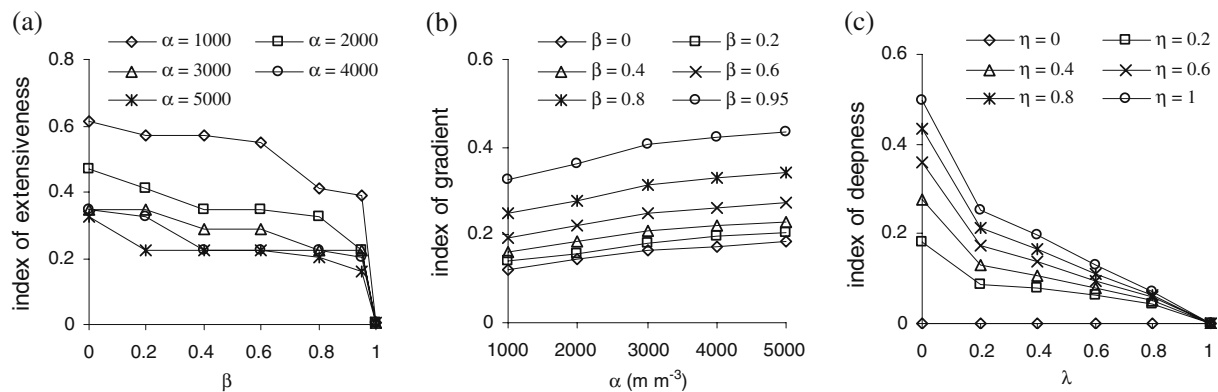


**Fig. 2** Two-dimensional interactions between architectural parameters in producing fine root distribution observed after 100 days of constant fine root dry matter (FRDM,  $\text{g day}^{-1}$ ) input of  $0.3 \text{ g day}^{-1}$  in a scene consisting of 196 cube voxels with  $0.1 \text{ m}$  length (four horizontal layers with  $7 \times 7$  voxels); root systems were initialised with  $0.1 \text{ m}$  of fine root length in the top central voxel; a permanent optimal soil condition was assumed with non-limiting water availability; FRDM input was measured on one-year old hybrid walnuts grown in a pot

experiment (data not published); the specific root length (SRL) was  $9.9 \text{ m g}^{-1}$  resulting in a fine root length increment of about  $3 \text{ m day}^{-1}$ ; the simulation results are synthesised with three indicators: **a** the proportion of rooted voxels in the simulation scene; **b** the ratio between standard deviation of root length density (zero densities for non-rooted voxels) obtained with a parameter setting and that obtained when colonisation process is not simulated; and **c** the proportion of total fine root in the two deeper horizontal layers

Efficiency of the parameter scaling rule to adjust for larger voxels

For different voxel shapes, adjusted  $\beta$  and  $\lambda$  values allow a very good prediction of root proportion at the stembase, 30 cm, 60 cm, and 90 cm lateral distance from the stembase compared to the reference fine root pattern (Fig. 4a). A less precise prediction of vertical root profiles however is produced when only the vertical size of the voxel is increased (Fig. 4b). The rate of decrease of root length density with depth is still underestimated with vertically stretched voxels. In all the other cases however, including inflated cubic voxels, the adjusted root profile provides good estimates of root proportion with depth. The parameter scaling rule shows a similar efficiency to adjust for larger voxels when predicting the coarse root patterns (data not shown).

Contrasting rooting systems of walnut and wild cherry

Figure 5 describes the spatial distribution of fine root density of walnut and wild cherry trees observed at the four harvest dates (May, June, August, and October) in four horizontal layers inside the pots. The presented values were the averages of two or three replications. In the first

harvesting date in May, 1 month after leaf emergence, no walnut root was found in the third and the fourth layer (Fig. 5a). In the next month, however, roots were found in the last layer. Root density increased in all layers between June and October. Roots of wild cherry trees were found in the third layer in May (Fig. 5b), 1.5 months after leaf emergence, and in the last layer starting from June. In the subsequent growing months, fine root density increased in all layers. Some walnut roots were observed to grow on the bottom and on the lateral pot boundary in August. More fine roots were found in October on the two pot boundaries but the number was negligible compared to that observed in the fourth layer or in the voxels situated near the lateral pot boundary. Some wild cherry roots were observed to grow on the lateral pot edge in August and on the pot bottom in October. At the early growing periods, both root systems of walnut and wild cherry trees developed more extensively in the second than in the first layer. In the last harvesting date, however, rooted areas were comparable between layers. Wild cherry roots were very concentrated in the second layer producing high root densities. In the last harvesting date, top layer root densities of wild cherry trees were higher than those of walnuts. There was no tendency that root system of both tree species grew toward a certain area inside pot.



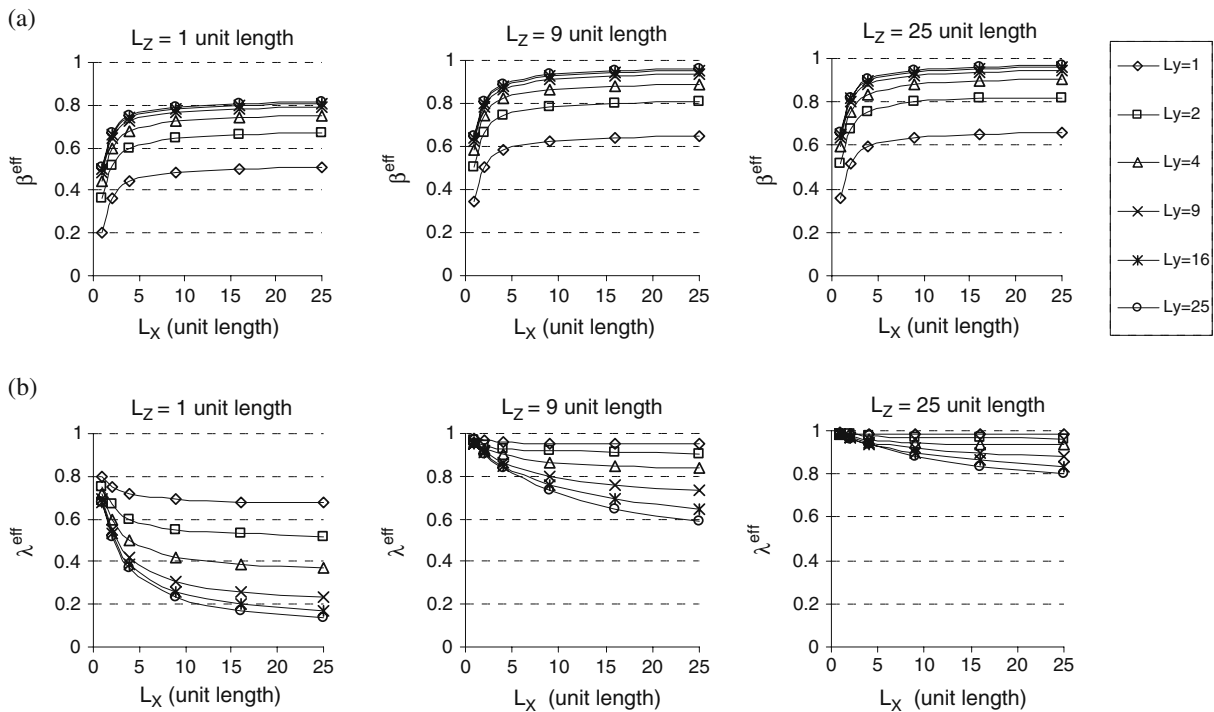


**Fig. 3** Example of adjusted  $\beta$  (a) and  $\lambda$  (b) values for different voxel shapes and sizes.  $\beta$  and  $\lambda$  are 0.2 and 0.8 respectively for a reference cubic voxel with a unit volume

We used a statistic proposed by Reddy and Pachepsky (2001) to test the difference between 3D fine root distribution patterns of the two tree species. This statistic compares within-species variation and between-species variation. The two species exhibit different root distribution patterns if the ratio between the two types of variation is greater than an F value. A significant difference was found ( $P < 0.05$ ) only at the end of the growing season in October. At the last uprooting date, the spatial root distribution of the two tree species showed differences related to gradient of root density and different preferential (vertical vs. horizontal) growth direction. Wild cherry exhibited a higher gradient of root density and higher preference for horizontal colonisation as observed in the first layer. As shown before (Fig. 2),  $\alpha$  and  $\beta$  govern the gradient of root density. The effect of  $\beta$  is however stronger than  $\alpha$  reflected by the values of gradient index. We therefore explored the effect of  $\beta$  and  $\lambda$  to explain the difference between the observed rooting patterns of the two tree species. We tested eleven values of  $\beta$  and  $\lambda$  between 0 and 1 with 0.1 interval. The simulations run with  $\alpha = 1,000 \text{ mm}^{-3}$ ,  $\eta = 0.8$ ,  $\varphi = 0.7$ , and  $\rho = 0$  for both tree species.

In the homogeneous substrate experiment, non-limited soil water availability in all voxels was assumed. In such conditions, we can assume that the potential water transport towards the roots was non-limiting and that the internal resistance to water transport inside the coarse roots was negligible. This means that the local water uptake is proportional to the local fine root length density (van Noordwijk and Lusiana 2000). Dry matter allocation to fine and coarse roots simulated with the root automata model can therefore be calculated as a function of the existing fine root length density.

To estimate  $\beta$  and  $\lambda$ , the square deviations between the observed and predicted fine root density were calculated. The smallest deviations were found when  $\beta$  and  $\lambda$  were around 0.3 and 0.6 respectively for walnut and 0.4 and 0.8 respectively for wild cherry root system. The predicted fine and total (fine + coarse) root densities with the selected parameter values were compared with the observed values (Fig. 6). A log-transformation was applied to reduce the variation of the voxel root density. The figure shows relatively good model predictions at the voxel scale for both walnut and wild cherry root densities. Some erratic values were however observed, as a

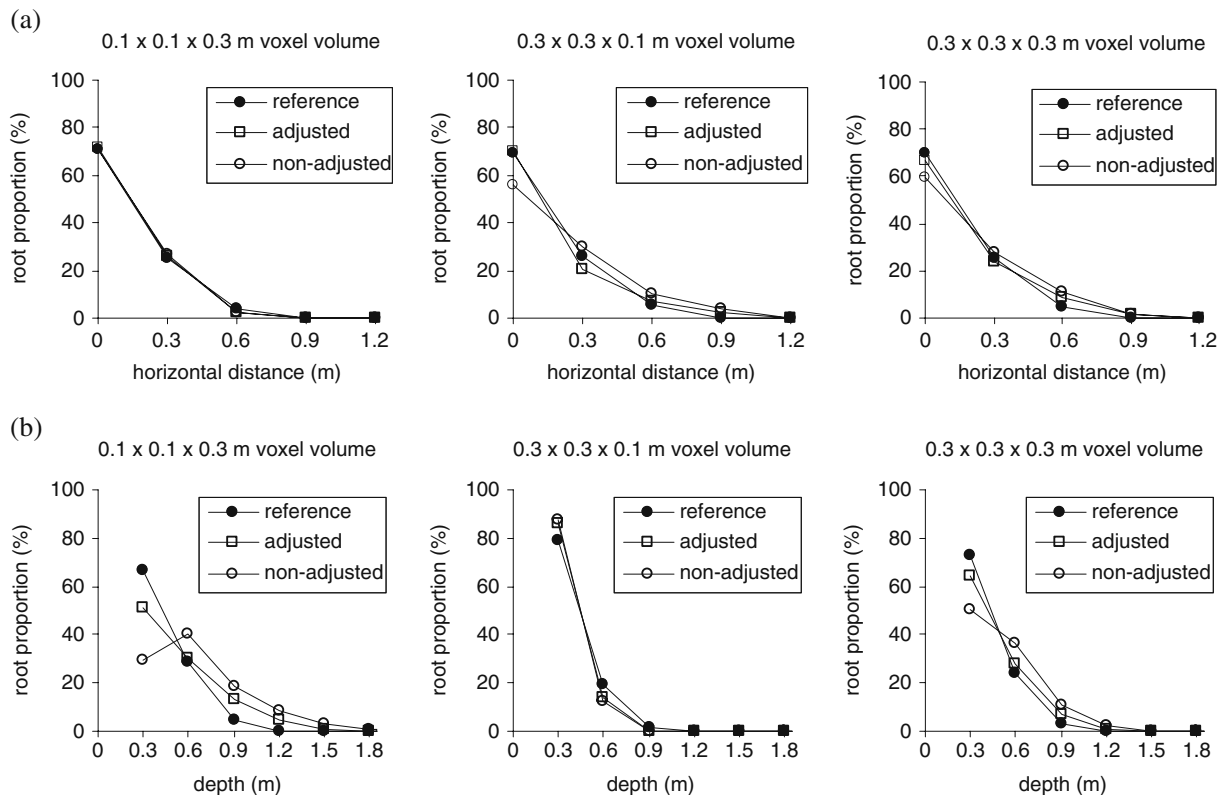


**Fig. 4** Effect of voxel shape and size on the predicted fine root distributions; the same 3 m cubic scene was compartmentalised in four different ways: i) 10 cm×10 cm×10 cm (in x, y, z direction respectively) small cubic voxels with the resulting root profiles as a reference, ii) 10 cm×10 cm×30 cm thick voxels, iii) 30 cm×30 cm×10 cm flat voxels, or iv) 30 cm×30 cm×30 cm large cubic voxels. In the scenario with larger voxels, the simulations were done with or without adjusted  $\beta$  and  $\lambda$  values; simulations with vertically stretched voxels were

done with a high vertical colonisation rate:  $\lambda=0.2$ ; those with horizontally stretched and inflated cubic voxels were run with a higher lateral colonisation rate, i.e.  $\lambda=0.8$  and  $\lambda=0.5$  respectively; the same values of  $\phi=0.5$ ,  $\rho=0.5$ ,  $\alpha=1,000 \text{ m m}^{-3}$ ,  $\beta=0.2$ , an  $\eta=1$  were applied for all simulations; each simulation was run for 730 days with constant FRDM inputs of  $0.3 \text{ g day}^{-1}$ ; root initialisation was done in the top central voxel with a fine root length of 0.1 m; soil condition was assumed to be optimal with non-limiting water availability

consequence of the patchy root observed distribution of the two species at the 10 cm scale in 3D. The significance of model's error was tested by the Reddy and Pachepsky statistic. The between-species variation was replaced however by the variation between predicted and observed root densities. No significance difference between observed and predicted root density was pronounced both for walnut and wild cherry ( $P>0.05$ ).

## Discussion

Hybrid cellular automata (e.g. Boswell et al. 2007; Sullivan and Knight 2004) are widely known as

efficient techniques to model processes interacting with the environment. Arvo and Kirk (1988) and Greene (1989) were the first to suggest using the cellular automata modelling approach to simulate plant growth by incorporating a control by the local environment. Such models are called environment-sensitive automata (Arvo and Kirk 1988) or voxel space automata (Greene 1989), and feature two innovative aspects: a) the lattice of cells (or 3D voxels) is no longer the object of simulation, but is rather a medium in which the objects of simulation themselves (e.g. plant roots) develop according to an automaton; b) interactions between the objects of simulation and the voxel environment are included (e.g. local soil condition). The locality

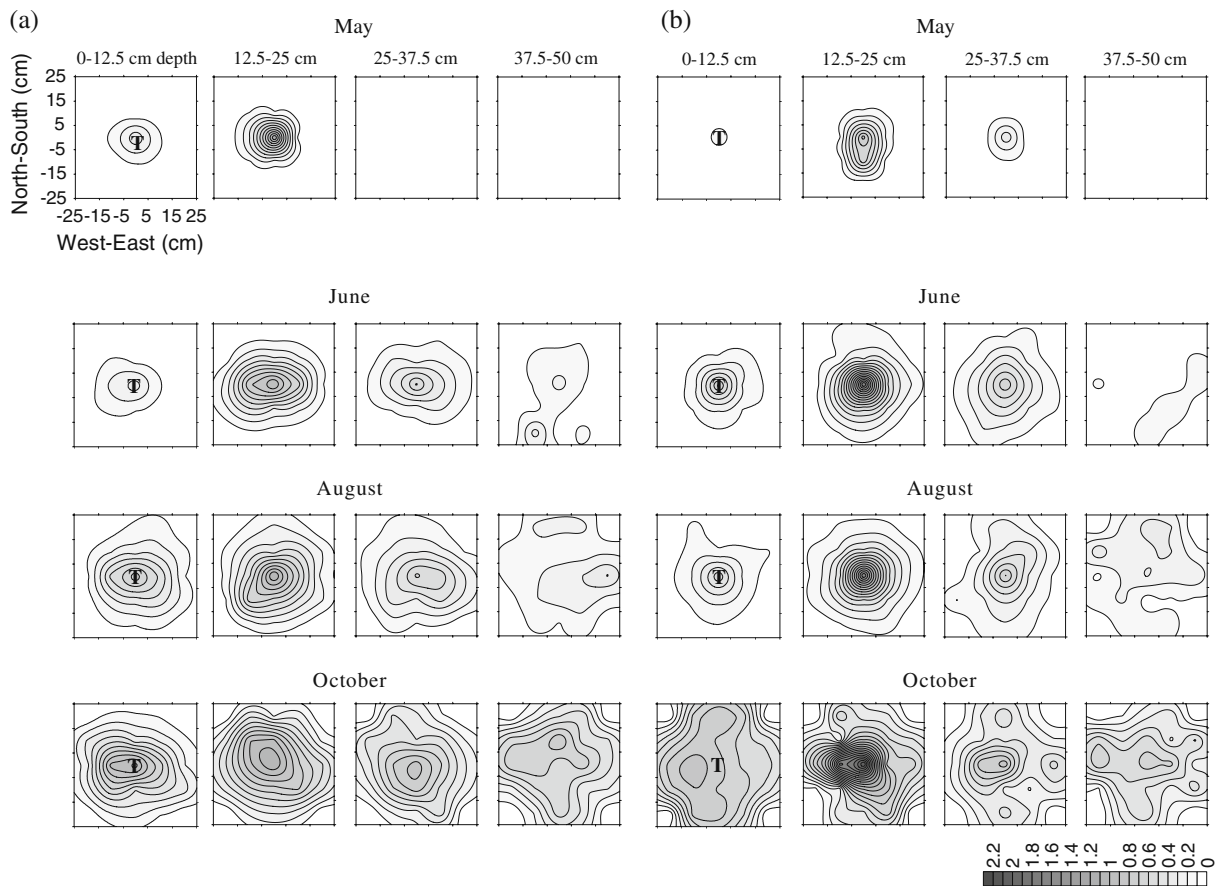


**Fig. 5** Distribution of observed fine root density ( $\text{kg m}^{-3}$ ) of walnut (a) and wild cherry (b) trees in the pots with an assumed uniform soil condition (water, penetrability, nutrient) observed at four harvest dates. The four successive maps at each date describe root distributions in the four successive horizontal

layers inside pot with depth. The letter 'T' indicates trunk position. The pot surfaces were indeed circular with diameter of 60 cm. The maps were made with SURFER (Golden Software Inc, Colorado, USA)

principle of the standard cellular automata approach that states that the transition rules of the automaton depend only on the state of the cell and of its neighbours is therefore no longer respected (Greene 1989). Greene (1991) and Wilderotter (2003) used the cellular automaton principle to model root growth but view the root system at the microscopic scale of individual roots.

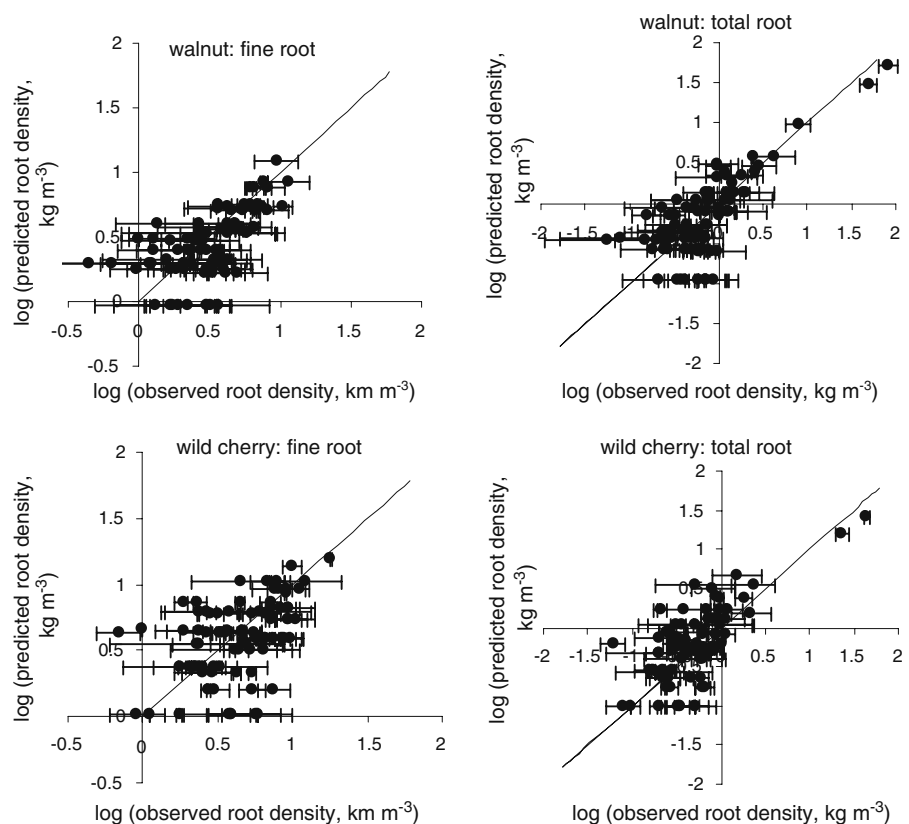
#### Voxel saturation of root density

The root model does not incorporate any limitation to the fine root density or the coarse root biomass in a voxel. The feed-back effect of resource depletion by an active fine root system is regarded as a feed-back process that prevents to predict unrealistic high root densities in a voxel. An exception may occur in a

voxel that is maintained in high resource conditions, such as under a drip irrigation nose and field observations confirm that extremely high root densities can be observed in such cases. Conversely, the coarse root biomass is not limited, and may increase indefinitely, especially for perennial plants such as trees. If small voxels are used, it could happen that the coarse root biomass in the voxel may occupy all the voxel volume. This is not an artefact as large coarse roots may effectively empty a voxel from the pre-existing soil.

Previously published root models include different hypotheses about a saturation threshold of root length density (Acock and Pachepsky 1996). Some authors consider that a maximum root concentration exists and growth ceases when such a limit is achieved. Other authors assume that root concentration does not

**Fig. 6** The predicted vs. observed root densities (log transformed) for fine and total (fine + coarse) root system of walnut and wild cherry trees with  $\beta=0.3$  and  $\lambda=0.6$  for walnut and  $\beta=0.4$  and  $\lambda=0.8$  for wild cherry. The solid lines indicate 1:1 relationship. The vertical bars indicate one standard error



limit root growth. In an optimal condition where soil resource availability is not limiting, we assume that root growth rate is not limited by root concentration. In natural conditions, root growth strongly depends on the local soil water conditions. Soil water availability in voxels with high root length densities may be rapidly depleted and the allocations of FRDM that are proportional to the local water uptake (i.e.  $\phi > 0$ ) would also rapidly reduce local root growth rate.

#### ‘Genetic $\times$ environment’ determined rooting patterns

Acock and Pachepsky (1996) defined a plagiotropism factor in dynamic root models as a preference for horizontal rather than vertical colonisation; others assume that the downward root extension does not have a deterministic vertical component and depends on the state of soil variables in the upper layers. The root voxel automaton may be parameterised to be fully opportunistic. If  $\lambda=0.67$  and  $\eta=0.5$ , the automaton has no preferential growth direction. In that case, the root growth will be governed only by local soil water conditions. Such a neutral architectural param-

eterisation may be used to test the relative importance of genetic and environment controls on root systems development. Many authors agree that the observed plant root distributions are the result of a genotype  $\times$  environment interaction, but the limited evidence of the role of genotype difference in plant root distribution may be due to the lack of suitable observation methods (van Noordwijk et al. 1996).

Hybrid walnut and wild cherry are two tree species with different habitat preferences. Walnut trees are reputed to thrive on deep alluvial soils and have deep tap-roots, while cherry trees have a more superficial tree root system and cannot face severe drought. We therefore expected different root growth behaviours between the two species, but it was not easy to predict if this would be true in perfectly uniform soil conditions as imposed in the homogeneous perlite substrate experiment. We ended up with different rooting patterns, reflected by different automaton parameters. This confirms the genetic control of the root system of young tree seedlings.

The root model can satisfactorily explain the difference in rooting behaviour between the two

species with two parameters. The values of other parameters were derived from published references. Since tree root systems are usually much less dense compared to crop's such as maize where Grant (1989) and Hayhoe (1981) used an  $\alpha$  value of  $2,500 \text{ m m}^{-3}$ , we proposed a value of  $1,000 \text{ m m}^{-3}$  for both tree species.  $\eta$  was considered as 0.8 for both walnut and wild cherry after observing the number of roots extending upward when uprooting the trees. Mulia (2005) estimated  $\phi$  equals 0.7 for hybrid walnut of the same species using a split root experiment. Due to the lack of data, the same value was applied for wild cherry. A zero value of  $\rho$  indicates that the effect of voxel-stembase distance to FRDM allocation was not verified with the pot experiment.

An upward extension of a root system is common and has been reported in the literature (e.g. Singh et al. 1989; von Carlowitz and Wolf 1991). It occurs for example with perennial root systems that are partially destroyed by superficial soil tillage. The ability of the tree root system to grow back upward determines the effectiveness of some root management options such as root pruning or the installation of root barriers. The effectiveness of such practices is reduced if tree roots can rapidly grow upward from beneath the root barrier or the tillage horizon. The root model is able to cope with these issues, and uses a topological voxel-stembase distance in all the algorithms that fully account for tortuous roots. Root barriers and root pruning may result in voxel-stembase distances that are much higher than the Euclidian distance.

### Increasing model complexity

It is well known that plant root systems are more developed in rich soil patches with higher water and/or nutrient concentration (De Jager 1985; Robinson 1994). This is regarded as an obvious foraging mechanism whereby plants compensate for the variability of soil, and adapt to inter-specific competition. The root automaton so far incorporates only the water extraction success control. This could be extended to include mineral capture success indicators. Pagès et al. (2000) reviewed existing models of plant root growth designed with continuum representation. They found that soil water content is the soil factor mostly considered by root models, followed by soil temperature, nitrogen and soil strength. The way of combining the effect of different soil factors is

however controversial: some models assume that the most limiting soil factor determines root growth (e.g. Asseng et al. 1997) while others take the additive or multiplicative effect of different soil factors (e.g. Addiscott and Whitemore 1987). Empirical evidence of hydraulic redistribution of soil water through tree root systems that connect wet and dry layers of soil (Bayala et al. 2008) adds further complexity and opportunities for positive and negative feedback in a model where dynamics of water and root development have a two-way linkage.

Another future important element of the root model will be the simulation of root decay, with consequences for the length of time fine roots can survive in dry soil zones as alternative to their re-emergence after rewetting of a soil layer (van Noordwijk et al. 1998). To our knowledge, three basic types of modelling root decay exist in the literature (van Noordwijk et al. 2004): either proportional to existing root length density according to a certain fraction, which leads to an exponential decay curve of surviving root length, based on a fixed lifespan of individual roots (varied between branching orders) and/or dominated by external environmental conditions. The soil factors determining the decay rate, however, vary between authors. In their review paper, Pagès et al. (2000) mentioned soil aeration, soil moisture and soil temperature as important soil factors, but also plant phenological stage, internal N level and plant water stress condition. In temperate regions, root death due to cold and anoxia are very important aspects of root system dynamics. We are currently incorporating the root decay process in the model. In the pot experiment, only at the final harvesting date we did observe very few dead roots. We therefore assumed that no root decayed during the experiment, resulting in good estimate of the actual root densities. It is well known that coarse root system provides both mechanical stability and water transport for the trees. Both plant internal and environmental factors influence the development coarse root system. Soil slope and external forces such as wind action influence the formation of tree coarse root system for mechanical stability (Coutts et al. 1999). The current model version only considers the function of coarse root system as the pathway for water transport. Modelling coarse root system that provides mechanical stability as well would be a challenge for the next version of the root model.

If a simulation of the root model starts with a rooted system that is occupying only one voxel, there is no need to initialise the coarse root biomass and topology. But if the simulation starts with a larger plant that colonise several voxels, it is necessary to initialise the coarse root system (both coarse root topology and biomass distribution). For a large plant, there are likely two ways to initialise the automaton: voxel by voxel (free root distribution pattern), or using an algorithm that generates a standard fine root distribution pattern with a given rooted volume (ellipsoidal, spherical or conical) and a pattern of fine root distribution within this volume (decreasing or uniform root densities with distance from the stem-base). A more difficult issue is to find a simple way to initialise coarse root topology of larger plants. Another challenging task will be to develop a 3D visualisation module that visualises the 3D coarse root topology. All these aspects of modelling extension will be considered for the next versions of the root model, but should not alter the two key advantages of voxel automata: its simplicity and the parsimonious number of parameters.

#### Potential model applications

Natural environment is usually patchy in every direction both above and belowground (Fitter et al. 2000; Hutchings and John 2004). It is particularly true in mixed cropping systems such as agroforestry where low-density tree stands grow with intercrops. In these systems, degree of heterogeneity increases due to uptakes of competing plants. A strong gradient of resources usually occurs between planting zones. An ‘unusual’ shape of plant root system might be found because roots have to adapt to a very patchy environment for successful resource uptakes. Within this shape, a negative exponential decrease of root density from the stembase as assumed by many plant root models is not respected; replaced by a root density distribution resulting from local response of the root system to resource availability (Mulia and Dupraz 2006). In all cropping systems, spatial soil resource heterogeneity occurs in case of rainfall that creates gradient of humidity between soil layers. Interception of tree canopy to rainfall also creates relatively lower soil humidity in areas below the canopy. In dry or sub-humid regions, superficial soil layers are usually very dry in summer and plant root

systems have to go deeper to access deep soil water for survival. An application of usual crop managements such as irrigation and fertilisation can also lead to a resource gradient between soil layers. Adaptive responses of root systems to their environment have much been shown by the result of different types of pot experiments. Some studies designed a horizontal or vertical soil resource gradient between pot compartments, and some applied a localised water or nutrient enrichment (e.g. Birch and Hutchings 1994). Root density distribution observed in these treatments is usually compared to those observed in a ‘control’ treatment. The root model assumes no predetermined hypothetical function of root distribution and allows roots to react to their local resource condition. Its continuum presentation allows an easy coupling with soil water balance and uptake models that are designed with a continuum presentation. It can estimate root distribution when foraging trait of root system is completely under influence of local resources or when a certain degree of genetic preference is assumed in the root colonisation process. A plot-scale model simulation with mature plants will however involve soil voxels with much bigger dimensions than used in the pot experiment for the model parameterisation. The values of  $\beta$  and  $\lambda$  for walnut and wild cherry were estimated with fine root densities measured on small voxels (10 cm scale). For a simulation with bigger voxel dimensions, the application of the scaling rule to compensate for the effect of voxel dimension is required. In the soil water balance and uptake models, voxel dimension is also taken into account in the calculation of soil water content in the voxels. When the root model is coupled with these models, the effect of voxel dimension will be considered both in the calculation of soil water content and of the value of architectural parameter  $\beta$  and  $\lambda$ . It is intriguing to investigate the interplay effect between soil water content, uptake and root growth when bigger or smaller voxel dimensions are applied. Studying the results of model applications in soils with different patterns of heterogeneity would be the next task.

#### Conclusion

It was a challenge to produce a dynamic root growth model that applies at the scale of the whole



plant, predicts the growth in 3D heterogeneous soil environments and still remains parsimonious in parameters. The suggested solution is an environment-sensitive automaton with only six parameters, and can easily be linked to a soil-water budget model and incorporated in a full plant or population model. These models are very intensive in calculations, and all previously existing 3D models of roots dynamics were unfortunately not usable in such models. This was a strong limitation to many studies in plant ecology or agronomy, including carbon sequestration (Woodward and Osborne 2000) studies or mixed cropping (Malézieux et al. 2008) studies where the dynamics of the below-ground part of the plants is often ignored. The proposed solution is a root model driven by the diffusion of fine roots across a medium compartmentalised in voxels, and linked by a coarse root system that is self-generated by the model. The ability of the model to generate a variety of rooting patterns in various soil conditions and to explain a contrasting rooting system of two temperate species was tested successfully. The main future development of the model will be the integration of more environmental controls on root growth (including mechanical resistance and aeration, both of which depend on soil water content) and simulation of root decay. Due to the flexibility of the root model in simulating the shape of a root system, the coupling of the root model with a tree-growth and soil-based model, or with a model simulating mixed system such as agroforestry stands will give new insight on how the root system of trees or competing plants grow and share resources available in heterogeneous soils.

**Acknowledgements** The model development and the pot experiments were part of the SAFE (Silvoarable Agroforestry for Europe) collaborative research project. SAFE was funded by the European Union under its Quality of Life programme, contract number QLK5-CT-2001-00560, and the support is gratefully acknowledged. We thank D. Harja (ICRAF, Bogor, Indonesia) and I. Lecomte (INRA, Montpellier, France) for their assistance in translating the modelling concepts to JAVA code.

**Open Access** This article is distributed under the terms of the Creative Commons Attribution Noncommercial License which permits any noncommercial use, distribution, and reproduction in any medium, provided the original author(s) and source are credited.

## References

- Acocck B, Pachepsky YaA (1996) Convective-diffusive model of two-dimensional root growth and proliferation. *Plant Soil* 180:231–240
- Addiscott TM, Whitemore AP (1987) Computer simulation of changes in soil mineral nitrogen and crop nitrogen during autumn, winter and spring. *J Agric Sci* 109:141–157
- Arvo J, Kirk D (1988) Modelling plants with environment-sensitive automata. *Proceedings of Ausgraph* 27–33
- Asseng S, Richter C, Wessolek G (1997) Modelling root growth of wheat as the linkage between crop and soil. *Plant Soil* 190:267–277
- Balandier P, Lacoite A, Le Roux X, Sinoquet H, Cruzat P, Le Dizès S (2000) SIMWAL: a structural-functional model simulating single walnut tree growth in response to climate and pruning. *Ann For Sci* 57:571–585
- Bayala J, Heng LK, van Noordwijk M, Ouedraogo SJ (2008) Hydraulic redistribution study in two native tree species of agroforestry parklands of West African dry savanna. *Acta Oecol* 34:370–378
- Birch CPD, Hutchings MJ (1994) Exploitation of patchily distributed soil resources by the clonal herb *Glechoma hederacea*. *J Ecol* 82(3):653–664
- Boswell G, Jacobs H, Ritz K, Gadd G, Davidson F (2007) The development of fungal networks in complex environment. *Bull Math Biol* 69(2):605–634
- Brugge R, Thornley JHM (1985) A growth model of root mass and vertical distribution, dependent on carbon substrate from photosynthesis and with non-limiting soil conditions. *Ann Bot* 55:563–577
- Clausnitzer V, Hopmans JW (1994) Simultaneous modelling of transient three-dimensional root growth and soil water flow. *Plant Soil* 164:299–314
- Coutts MP, Nielsen CCN, Nicoll BC (1999) The development of symmetry, rigidity and anchorage in the structural root system of conifers. *Plant Soil* 217:1–15
- De Jager A (1985) Response of plants to a localized nutrient supply. PhD Thesis, University of Utrecht, pp 137
- De Willigen P, Heinen M, Mollier A, van Noordwijk M (2002) Two-dimensional growth of a root system modelled as a diffusion process. I. Analytical solutions. *Plant Soil* 240:225–234
- Diggle AJ (1988) ROOTMAP: a model in three-dimensional coordinates of the growth and structure of fibrous root system. *Plant Soil* 105:169–178
- Doussan C, Pagès L, Pierret A (2003) Soil exploration and resource acquisition by plant roots: an architectural and modelling point of view. *Agronomie* 23:419–431
- Dunbabin V, Diggle AJ, Rengel Z, van Hungten R (2002a) Modelling the interactions between water and nutrient uptake and root growth. *Plant Soil* 239:19–38
- Dunbabin V, Diggle AJ, Rengel Z (2002b) Simulation of field data by a basic three-dimensional model of interactive root growth. *Plant Soil* 239:39–54
- Fitter A, Hodge A, Robinson D (2000) Plant response to patchy soils. In: Hutchings MJ, John EA, Stewart AJA (eds) *The ecological consequences of environmental heterogeneity*. British Ecological Society, Blackwell Ltd, Oxford, pp 71–90

- Grant RF (1989) Simulation of carbon assimilation and partitioning in maize. *Agron J* 81:563–571
- Greene N (1989) Voxel space automata: modelling with stochastic growth processes in voxel space. *Comput Graph* 23:175–184
- Greene N (1991) Detailing tree skeletons with voxel automata. Siggraph course notes for photorealistic volume modelling and rendering technique 1–15
- Hayhoe H (1981) Analysis of a diffusion model for plant root growth and an application to plant soil-water uptake. *Soil Sci* 131:334–343
- Heinen M, Mollier A, De Willigen P (2003) Growth of a root system described as diffusion. II. Numerical model and application. *Plant Soil* 252:251–265
- Hillel D, Talpaz H (1976) Simulation of root growth and its effect on the pattern of soil water uptake by a non-uniform root system. *Soil Sci* 121:307–312
- Hutchings MJ, John EA (2004) The effects of environmental heterogeneity on root growth and root/shoot partitioning. *Botanical briefing. Ann Bot-London* 94:1–8
- Jones CA, Bland WL, Ritchie JT, Williams JR (1991) Simulation of root growth. In: Hanks J, Ritchie JT (eds) *Modelling plant and soil systems*. Madison: Agronomy Monograph 31, 91–124
- Lacointe A (2000) Carbon allocation among tree organs: a review of basic processes and representation in functional-structural tree models. *Ann For Sci* 57:521–533
- Lacointe A, Isebrands JG, Host GE (2002) A new way to account for the effect of source-sink spatial relationships in whole plant carbon allocation models. *Can J For Res* 32:1838–1848
- Le Roux X, Lacointe A, Escobar-Gutiérrez A, Le Dizès S (2001) Carbon-based models of individual tree growth: a critical appraisal. *Ann For Sci* 58:469–506
- Malézieux E, Crozat Y, Dupraz C, Laurans M, Makowski D, Ozier-Lafontaine H, Rapidel B, de Tourdonnet S, Valantin-Morison M (2008) Mixing plant species in cropping systems: concepts, tools and models. A review. *Agron Sustain Dev* 28:1–20
- Mobbs DC, Lawson GJ, Friend AD, Crout NMJ, Arah JRM, Hodnett MG (1999) HyPAR: Model for agroforestry systems. Technical manual. Model description for version 3.0. Penicuik, Scotland: Institute of Terrestrial Ecology 44–45
- Mulia R (2005) 3D modelling of the growth of plant root systems in heterogeneous soils with voxel automata approach—Modelling concept and application with agroforestry trees. PhD Thesis, University of Montpellier II, pp 87
- Mulia R, Dupraz C (2006) Unusual fine root distributions of two deciduous tree species in southern France: what consequences for modelling of tree root dynamics? *Plant Soil* 281:71–85
- Page ER, Gerwitz A (1974) Mathematical models, based on diffusion equation, to describe root systems of isolated plants, row crops, and swards. *Plant Soil* 41:243–254
- Pagès L, Asseng S, Pellerin S, Diggle A (2000) Modelling root system growth and architecture. In: Smit AL, Bengough AG, Engels C, van Noordwijk M, Pellerin S, van De Geijn SC (eds) *Root methods*. Springer-Verlag, Berlin, pp 113–146
- Reddy VR, Pachepsky YaA (2001) Testing a convective-dispersive model of two dimensional root growth and proliferation in a greenhouse experiment with maize plants. *Ann Bot* 87:759–768
- Robinson D (1994) The responses of plants to non uniform supply of nutrients. *New Phytol* 127:635–674
- Singh RP, Ong CK, Saharan N (1989) Above and below ground interactions in alley-cropping in semi-arid India. *Agroforest Syst* 9:259–274
- Somma F, Hopmans JW, Clausnitzer V (1998) Transient three-dimensional modelling of soil water and solute transport with simultaneous root growth, root water, and nutrient uptake. *Plant Soil* 202:281–293
- Sullivan AL, Knight IK (2004) A hybrid cellular automata/semi-physical model of fire growth. *Proc Conf Complex Systems* 64–73
- van Noordwijk M, De Willigen P (1986) Quantitative root ecology as element of soil fertility theory. *Neth J Agric Sci* 34:273–281
- van Noordwijk M, Brouwer G (1991) Review of quantitative root length data in agriculture. In: Persson H, McMichael BL (eds) *Plant roots and their environment*. Elsevier, Amsterdam, pp 515–525
- van Noordwijk M, Lusiana B (2000) Background on a model of water, nutrient, and light capture in agroforestry systems. ICRAF, Bogor, pp 54–55
- van Noordwijk M, Cadisch G (2002) Access and excess problems in plant nutrition. *Plant Soil* 247:25–39
- van Noordwijk M, Mulia R (2002) Functional branch analysis as tool for scaling above- and belowground trees for their additive and non-additive properties. *Ecol Modell* 149:41–51
- van Noordwijk M, Lawson G, Soumaré A, Groot JJR, Hairiah K (1996) Root distribution of trees and crops: competition and/or complementarity. In: Ong CK, Huxley P (eds) *Tree-crop interaction*. CAB International, Wallingford, pp 319–364
- van Noordwijk M, Martikainen P, Bottner P, Cuevas E, Rouland C, Dhillon SS (1998) Global change and root function. *Glob Chang Biol* 4:759–772
- van Noordwijk M, Rahayu S, Williams SE, Hairiah K, Khasanah N, Schroth G (2004) Crop and tree root-system dynamics. In: van Noordwijk M, Cadisch G, Ong CK (eds) *Belowground interactions in tropical agroecosystems*. CAB International, Wallingford, pp 83–107
- von Carlowitz PG, Wolf GV (1991) Open-pit sunken planting: a tree establishment technique for dry environments. *Agroforest Syst* 15:17–29
- Wilderotter O (2003) An adaptive numerical method for the Richards equation with root growth. *Plant Soil* 251:255–267
- Woodward FI, Osborne CP (2000) The representation of root processes in models addressing the responses of vegetation to global change. *New Phytol* 147:223–232